Published OnlineFirst May 12, 2009; DOI: 10.1158/0008-5472.CAN-08-4645

Rapamycin Prevents Early Onset of Tumorigenesis in an Oral-Specific K-*ras* and *p53* Two-Hit Carcinogenesis Model

Ana R. Raimondi, Alfredo Molinolo, and J. Silvio Gutkind

Oral and Pharyngeal Cancer Branch, National Institute of Craniofacial and Dental Research, NIH, Bethesda, Maryland

Abstract

Head and neck squamous cell carcinomas (HNSCC), the majority of which occur in the oral cavity, remain a significant cause of morbidity and mortality worldwide. A major limitation in HNSCC research has been the paucity of animal models to test the validity of current genetic paradigms of tumorigenesis and to explore the effectiveness of new treatment modalities and chemopreventive strategies. Here, we have developed an inducible oral-specific animal tumor model system, which consists in the expression of a tamoxifen-inducible Cre recombinase (CreER^{tam}) under the control of the cytokeratin 14 (K14) promoter (K14-CreER^{tam}) and mice in which the endogenous K-*ras* locus is targeted (LSL-K-*ras*^{G12D}), thereby causing the expression of endogenous levels of oncogenic K-*ras*^{G12D} following removal of a stop element. Surprisingly, whereas K14-CreER^{tam} can also target the skin, K14-CreER^{tam}/LSL-K-*ras*^{G12D} mice developed papillomas exclusively in the oral mucosa within 1 month after tamoxifen treatment. These lesions were highly proliferative but never progressed to carcinoma. However, when crossed with *p53* conditional knockout (*p53*$^{flox/flox}$) mice, mice developed SCCs exclusively on the tongue as early as 2 weeks after tamoxifen induction, concomitant with a remarkable activation of the mammalian target of rapamycin (mTOR) signaling pathway. The availability of this *ras* and *p53* two-hit animal model system recapitulating HNSCC progression may provide a suitable platform for exploring novel molecular targeted approaches for the treatment of this devastating disease. Indeed, we show here that mTOR inhibition by the use of rapamycin is sufficient to halt tumor progression in this genetically defined oral cancer model system, thereby prolonging animal survival. [Cancer Res 2009;69(10):4159–66]

Introduction

Head and neck squamous cell carcinomas (HNSCC), the vast majority of which occur in the oral cavity, remain a significant cause of morbidity and mortality worldwide (1), resulting in more than 10,000 deaths each year in the United States alone (2). Like most cancers, HNSCC progression involves the sequential acquisition of genetic and epigenetic alterations in tumor suppressor genes and oncogenes (reviewed in ref. 3). The most frequent alterations include loss of heterozygosity and promoter silencing of the *p16* and inactivating mutations in the *p53* tumor suppressor genes (3). HNSCC often overexpress the epidermal growth factor receptor and some of its active variants (4) and harbor activating mutations in the *ras* oncogene with a rate ranging from 3% to 5% in Western countries and up to 50% in India and Southeast Asia (5–7).

Advances in the understanding of the molecular mechanisms involved in HNSCC have been hampered by the limited availability of appropriate animal models for oral malignancies. In this regard, genetically engineered mouse models are powerful tools to investigate specific cause and effect relationships between molecular changes and cancer development and progression (8). However, the use of genetically defined approaches for HNSCC has been limited due to the lack of specific systems targeting the oral stratified epithelium. For example, expression of the K-*ras* oncogene in the oral epithelium under the control of a cytokeratin 5 (K5) promoter-driven *tet*-on inducible system leads to SCC in the oral mucosa and the salivary glands, skin, and other squamous epithelia (9, 10). A K5 promoter-driven Cre recombinase system that is activated by the local administration of a synthetic progesterone derivative has been used to express a mutant K-*ras* allele in the oral epithelium of mice, leading to the development of oral benign papillomas (11). These mice develop massive oral carcinomas when crossed with animals lacking transforming growth factor receptor II (TGFβRII); therefore, they are no longer responsive to the growth-suppressive activity of TGFβ (7). In these conditional TGFβRII$^{-/-}$ mice (7), progression to SCC was achieved by the use of chemical carcinogens, likely promoting *ras* mutations. Thus, we have explored additional approaches to achieve the development of malignant lesions in a genetically defined cancer cell autonomous-driven model, which may therefore facilitate recapitulating oral tumorigenesis.

We show here that mice expressing a tamoxifen-inducible Cre recombinase under the control of the cytokeratin 14 (K14) promoter (K14-CreER^{tam}) and the *ras* oncogene from its own promoter after Cre excision of a stop signal (LSL-K-*ras*^{G12D} mice) develop large papillomas exclusively in the oral cavity and hyperplasia in the tongue within 1 month of a tamoxifen treatment. Furthermore, if these mice are crossed with floxed *p53* conditional knockout (p53$^{flox/flox}$) mice, the compound mice develop carcinomas exclusively on the tongue as early as 2 weeks after tamoxifen induction. The use of this K14-CreER^{tam}/LSL-K-*ras*$^{G12D/+}$/p53$^{flox/flox}$ animal model may help recapitulate oral cancer progression in a genetically defined two-hit system involving *ras* activation and *p53* inactivation, thus facilitating the study of the molecular mechanisms underlying HNSCC progression. In this regard, we show that the activation of the mammalian target of rapamycin (mTOR) signaling pathway is an early event in both oral benign and malignant lesions and that targeting mTOR by the use of rapamycin halts tumor progression in this genetically defined oral cancer model, thereby prolonging animal survival.

Note: Supplementary data for this article are available at Cancer Research Online (http://cancerres.aacrjournals.org/).

Requests for reprints: J. Silvio Gutkind, Oral and Pharyngeal Cancer Branch, National Institute of Craniofacial and Dental Research, NIH, 30 Convent Drive, Building 30, Room 211, Bethesda, MD 20892-4340. Phone: 301-496-6259; Fax: 301-402-0823; E-mail: sg39v@nih.gov.

doi:10.1158/0008-5472.CAN-08-4645

Published OnlineFirst May 12, 2009; DOI: 10.1158/0008-5472.CAN-08-4645

Materials and Methods

Generation of mice with K-*ras*^{G12D} activation and p53 deletion. Mouse strains, K14-CreER^{tam} (The Jackson Laboratory), LSL-K-*ras*^{G12D}, and p53$^{flox/flox}$, have been described (12–14). Their genetic backgrounds were as follows: K14-CreER^{tam} and p53$^{flox/flox}$, FVB/N; LSL-K-*ras*^{G12D}, 129Sv. K14-CreER^{tam} mice were crossed with LSL-K-*ras*$^{G12D/+}$ mice to generate K14-CreER^{tam}/LSL-K-*ras*$^{G12D/+}$ mice and subsequently bred with p53$^{flox/flox}$ mice to generate K14-CreER^{tam}/LSL-K-*ras*^{G12D}/p53$^{flox/+}$ mice. These mice were further crossed with p53$^{flox/flox}$ to generate K14-CreER^{tam}/LSL-K-*ras*^{G12D}/p53$^{flox/flox}$ line. K14-CreER^{tam} mice were also crossed to Rosa26-LacZ homozygous reporter mice to generate K14-CreER^{tam}/Rosa26-LacZ mice. K14-CreER^{tam} mice were used as heterozygous in all the lines established. Tamoxifen was administered to 1-mo-old animals, 1 mg/mouse/d orally, for 5 consecutive days. Control mice received only the tamoxifen solvent (sunflower oil) with the same schedule. Genotyping was performed on tail biopsies by PCR using specific primers (12–14). Excision of the stop cassette from the LSL-K-*ras*^{G12D} allele was determined in DNA purified from tissues of wild-type and the indicated compound mice treated with or without tamoxifen using the following primers: 5′-GGGTAGGTGTTGGGATAGCTG-′1 and 3′-TCCGAATT-CAGTGACTACAGATGTACAGAG-3′ (sequence obtained from Dr. Tyler Jacks laboratory, Koch Institute at MIT, Cambridge, MA). Cre-mediated recombination of the p53 floxed allele was confirmed as previously described (14). All experiments involving mice were carried out according to NIH-approved protocols, in compliance with the Guide for the Care and Use of Laboratory Animals.

Rapamycin administration. Rapamycin (LC Laboratories) was diluted in aqueous solution of 5.2% Tween 80 (Sigma) and 5.2% polyethyleneglycol (PEG-400; Hampton Research), as previously described (15), and injected i.p. at a final dose of 10 mg/kg every other day.

Histology, histochemistry, immunohistochemistry, and Western blotting. One hour before euthanasia, mice were injected i.p. with 5′-bromo-2′-deoxyuridine (BrdUrd; 100 μg/g body weight) for cell proliferation assays. All tumor lesions and control tissues were dissected, fixed overnight in buffered 4% paraformaldehyde at room temperature, dehydrated, and embedded in paraffin. H&E-stained sections were used for diagnostic purposes, and unstained serial sections for immunohistochemical studies. Immunohistochemistry was performed as previously described (10). Western blots were performed on lysates from frozen tissues. Protein concentration was determined, and 50 μg of total proteins were separated on SDS-PAGE, transferred to nitrocellulose membranes, and blocked with 5% dry milk. Antibodies used include cyclin D1 (92G2), phospho-S6 ribosomal protein Ser$^{240/244}$ (pS6), and phospho-p44/42 mitogen-activated protein kinase (MAPK) Thr^{202}/Tyr^{204} (pMAPK 9101) from Cell Signaling Technology; and cytokeratin 1 (MK1; Covance); antibodies to proliferating cell nuclear antigen (PCNA; Zymed), BrdUrd (Biogenex), tubulin, MAPK (extracellular signal-regulated kinase 1/2), and DUSP-14/MKP-6 (Santa Cruz Biotechnology) were also used. The antibodies for K14 and filaggrin were kindly provided by Dr. J. Segre (National Human Genome Research Institute, NIH, Bethesda, MD). β-Galactosidase histochemistry was performed on cryostat section from snap-frozen OCT-embedded tissue samples (10). Terminal deoxynucleotidyl transferase–mediated dUTP nick end labeling (TUNEL) assay was performed using the *In Situ* Cell Death Detection kit, AP (Roche) according to the manufacturer's instructions. The evaluation of the immunohistochemistry was conducted blindly, without knowledge of the origin and genotype. Tissues were classified based on the staining intensity (0, no staining; 1, weak staining; 2, moderate staining; and 3, strong staining) and the percentage of positive cells (0, between 0% and 25% of stained cells; 1, between 25% and 50%; 2, between 50% and 75%; 3, between 75% and 100% of cells stained). Results were scored by multiplying the percentage of positive cells by the intensity, as previously described (16).

Hierarchical clustering and data visualization. The staining scores that resulted from immunohistochemistry were converted into scaled values centered on zero, and hierarchical analysis was performed using Cluster program[1] with average linkage based on Pearson's correlation coefficient as the selection parameter on the unsupervised approach. The results were visualized using the Java TreeView software. The clustered data were arranged with markers on the horizontal axis and tissue samples on the vertical axis as recently described (16). Two biomarkers with a close relationship are located next to each other.

Statistical analysis. Kaplan-Meier survival curves and its statistical analysis, as well as log-rank test followed by a post hoc comparison (Holm-Sidak test), were performed using the SigmaStat software package.

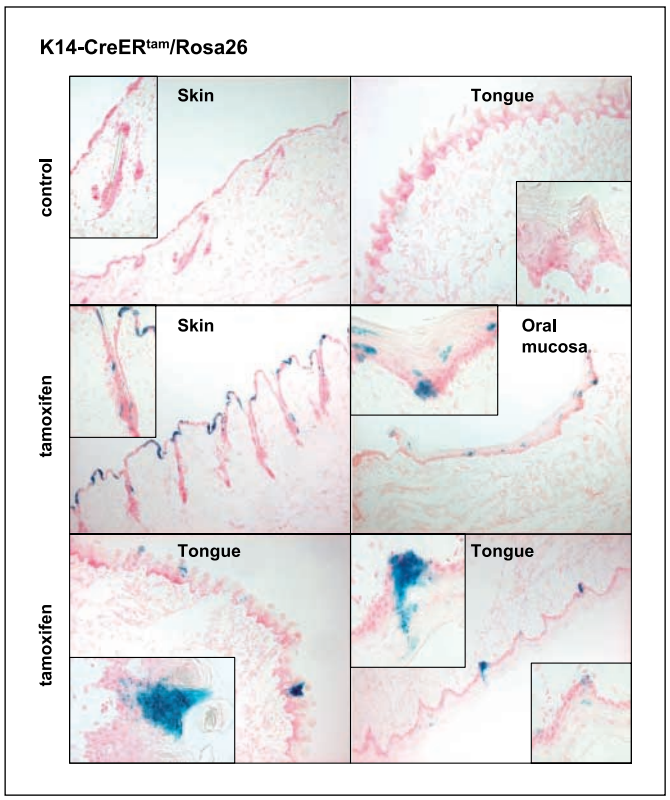

Figure 1. The K14-CreER^{tam} expression system enabled the Cre-mediated recombination in the oral cavity. The double K14-CreER^{tam}/Rosa26-LacZ transgenic mice were treated with tamoxifen or solvent (control) orally during 5 consecutive days. Skin, oral mucosa, and tongue biopsies were taken 1 mo after treatment. β-Galactosidase activity was readily detected in the interfollicular epidermis and hair follicles. The oral cavity showed scattered positive cells on the oral mucosa and the epithelial basal layer of the tongue. Dorsal and ventral tongue presented β-galactosidase in columns of positive cells on the entire epithelium. Magnifications, ×20 (original) and ×40 (insets).

Results

Development of tumoral oral lesions on tamoxifen-induced *ras* activation in K14-CreER^{tam}/LSL-K-*ras*$^{G12D/+}$ mice. We explored the consequences of targeting *ras* to the basal layer of the oral mucosa and tongue by examining whether mice expressing a tamoxifen-inducible form of Cre recombinase under the control of the K14 promoter (17) could induce Cre/LoxP-mediated recombination when crossed with the Rosa26 reporter animal line. The administration of tamoxifen to K14-CreER^{tam}/Rosa26-LacZ mice resulted in the expression of β-galactosidase in epithelial cells within the interfollicular skin, hair follicle, and bulge region of the hair follicle (Fig. 1), as previously reported (12). Of interest, these mice also expressed β-galactosidase in scattered cell populations in the epithelium lining the tongue (12) and oral mucosa (Fig. 1) but

[1] http://rana.lbl.gov/EisenSoftware.htm

Published OnlineFirst May 12, 2009; DOI: 10.1158/0008-5472.CAN-08-4645

not when treated with the vehicle (Fig. 1). Thus, this system enabled the inducible Cre-mediated recombination of sporadic cells within the oral cavity, likely involving the epithelial stem cell population, as groups or columns of β-galactosidase–positive cells initiated at the basal layer were visible beyond 1 month after tamoxifen treatment in both the tongue and oral mucosa, in spite of the rapid turnover of the oral epithelial cells (Fig. 1).

Members of the *ras* oncogene family (H-*ras*, K-*ras*, and N-*ras)* are often mutated in human cancer (18, 19). A high incidence of *ras* mutations occurs in Southeast Asia, where it is associated with areca nut chewing, but much less frequently mutated in the Western countries (5, 20, 21). The use of the LSL-K-*ras*^{G12D} strain that enables achieving endogenous levels of oncogenic K-Ras^{G12D} protein on the removal of the stop element (13) by the K14-CreER^{tam}–mediated recombination led to the developed large exophytic tumors exclusively in the oral mucosa in all mice studied as early as 1 month after the tamoxifen induction (n = 18; Fig. 2). In contrast, a group of K14-CreER^{tam} and LSL-K-*ras*$^{G12D/+}$ mice treated with tamoxifen and control K14-CreER^{tam}/LSL-K-*ras*$^{G12D/+}$ animals treated with solvent alone did not develop any lesions or exhibit any differences in survival rate (Fig. 3 and data not shown). Tumors arising in tamoxifen-treated K14-CreER^{tam}/LSL-K-*ras*$^{G12D/+}$ mice were hyperkeratotic squamous cell papillomas (Fig. 2). Increased cell proliferation, restricted to the basal layers (Fig. 2), was coupled with cell differentiation, as judged by the positive immunostaining for filaggrin (Fig. 2). We observed, however, changes in the pattern of expression of cytokeratins. For example, K14 was expressed poorly in the basal layer but strongly in the upper layers of the papillomas, different from its distribution in normal epithelium (Fig. 2) but similar to that observed in chemically induced skin papillomas (22). On the other hand, K1 was expressed in the upper layers of the hyperplastic epithelium but not in the control normal oral mucosa (Fig. 2). The majority of the tongues showed a marked hyperplasia with significant acanthosis, papillomatosis, and hyperkeratosis (Fig. 2). No animals developed carcinomas, but they had to be sacrificed 2 to 3 months after tamoxifen administration, as these lesions exceeded acceptable size and thus compromised food intake (Fig. 3).

We confirmed that the treatment with tamoxifen leads to the CreER^{tam}-dependent recombination of the LSL-K-*ras*^{G12D} allele

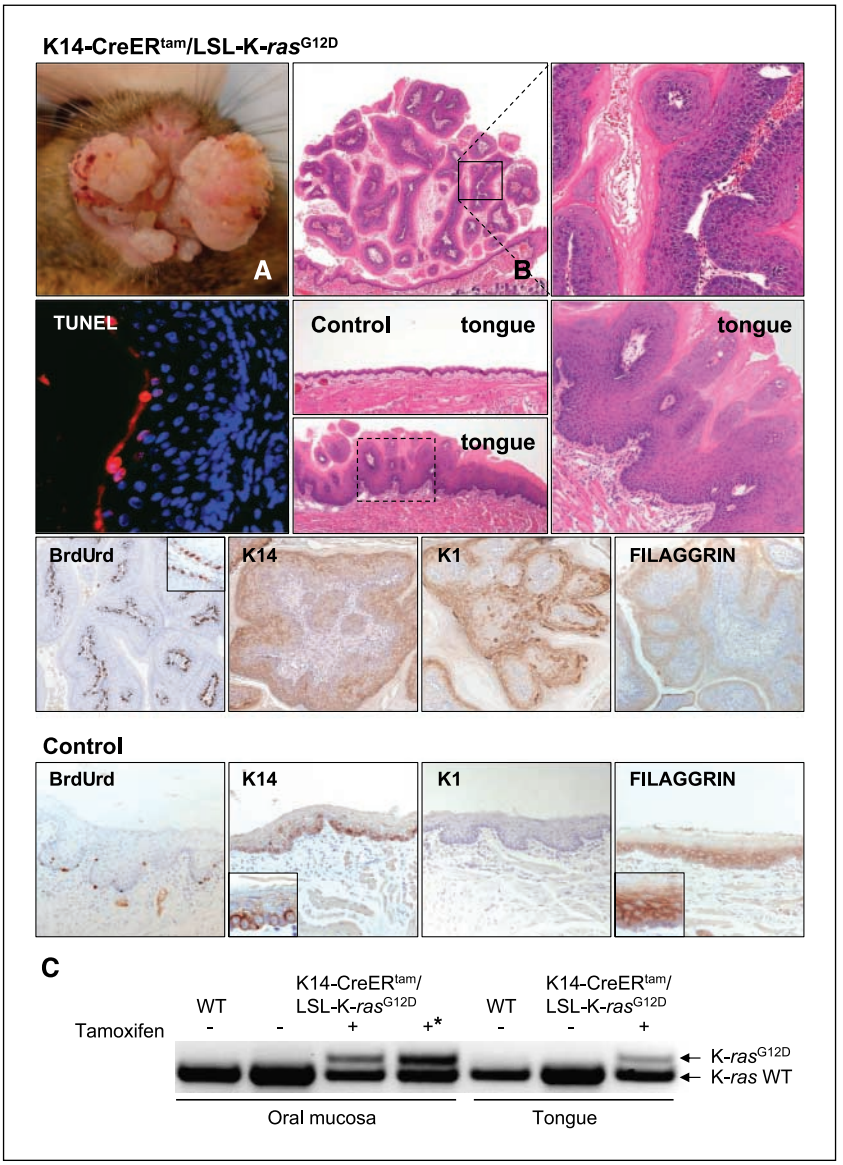

Figure 2. K14-CreER^{tam}/SL-K-*ras*$^{G12D/+}$ mice develop squamous papillomas in the oral mucosa on tamoxifen treatment. *A,* papillomas arising from the oral mucosa of K14-CreER^{tam}/SL-K-*ras*^{G12D} mice on tamoxifen treatment were characterized by exophytic growth. *B,* hyperplastic epithelium covering thin stromal finger-like projections that grow out of the oral squamous epithelium. Typical features include hyperkeratosis and the presence of hyperplastic, well-differentiated squamous epithelium with few apoptotic cells in the upper layers (TUNEL reaction). Normal (*control*) tongue epithelium is clearly different in control animals when compared with a highly hyperplastic area in K14-CreER^{tam}/LSL-K-*ras*$^{G12D/+}$ mice (below *control*). In these tumors, BrdUrd incorporation is restricted to the basal layers (detail in *inset*), and there is a deregulated expression of K14; the normal expression pattern is inverted in tumoral lesions, with enhanced expression in suprabasal keratinocytes. The expression of K1 is irregular but limited to the upper layers of the hyperplastic epithelium. The upper layers of the papillomas express filaggrin, a differentiation marker. In normal control mucosa, K14- and BrdUrd-positive cells are seen in the basal layer. No staining with K1 is evident in this oral mucosa and the expression of filaggrin is observed only in the upper layers. *C,* PCR analysis with primers that flank the stop cassette in the LSL-K-*ras*^{G12D} allele using purified DNA from the oral mucosa and tongue of mice treated (+) or not (–) with tamoxifen in the indicated genetic backgrounds. LSL-K-*ras*^{G12D} allele recombination occurred only in the oral mucosa of the K14-CreER^{tam}/LSL-K-*ras*$^{G12D/+}$ mice on tamoxifen induction. *, DNA isolated from a papilloma. The hyperplastic tongue of K14-CreER^{tam}/LSL-K-*ras*$^{G12D/+}$ mice also showed excision of the stop cassette after Cre activation by tamoxifen treatment.

Published OnlineFirst May 12, 2009; DOI: 10.1158/0008-5472.CAN-08-4645

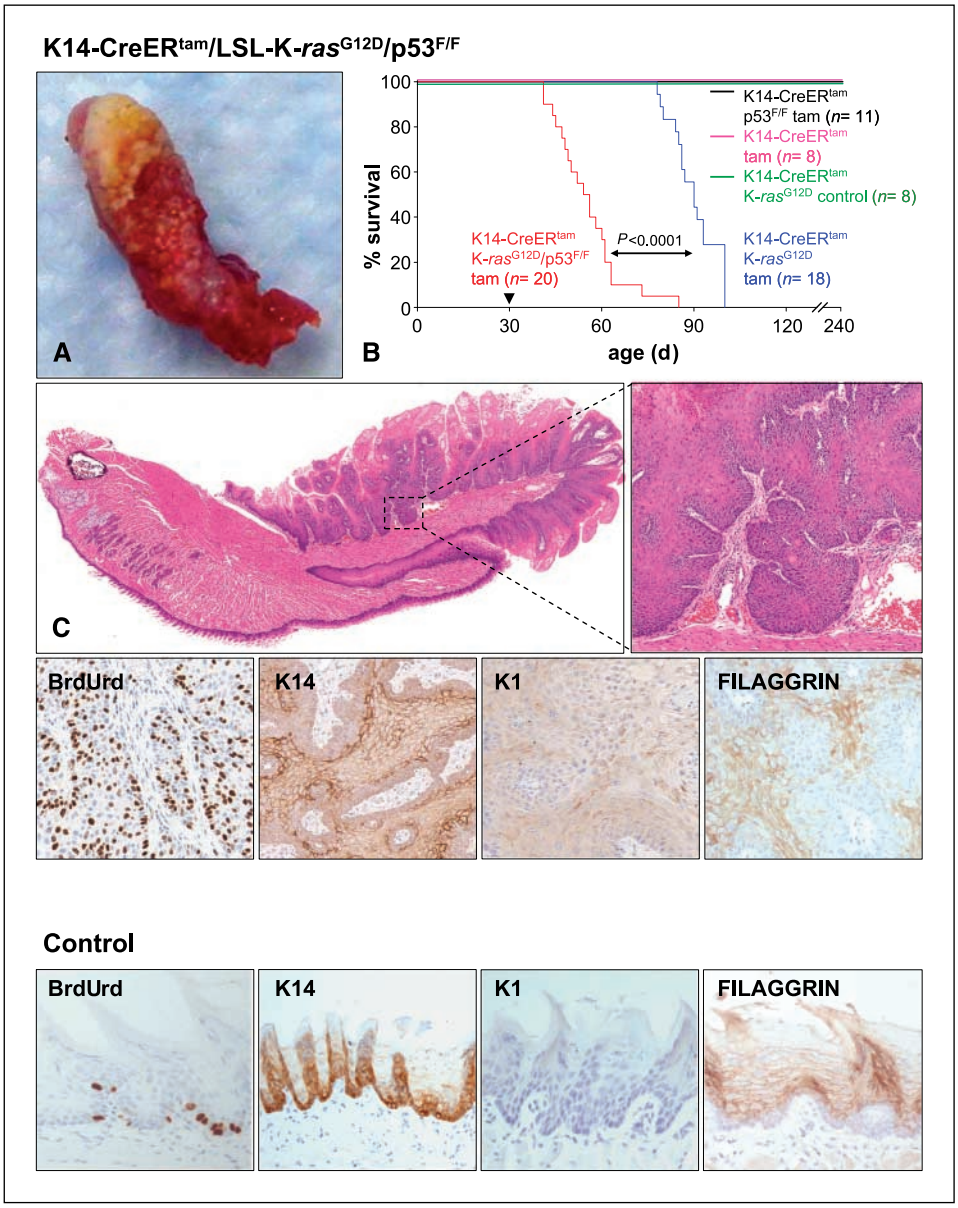

Figure 3. Tongue squamous carcinoma formation in K14-CreER^{tam}/LSL-K-*ras*$^{G12D/+}$/p53$^{flox/flox}$ mice. *A,* gross appearance of a carcinoma of the tongue from a compound mouse after tamoxifen treatment. The yellowish area of the ventral area of the tongue corresponds to the carcinoma. *B,* Kaplan-Meier survival curve of the indicated mice lines treated (*tam*) or not (*control*) with tamoxifen. The combination of expression of K-*ras*^{G12D} with the lack of a functional *p53* (*K-ras*^{G12D}/*p53*$^{F/F}$ *tam*) resulted in a statistically significant decreased survival rate when compared with mice expressing an activated *ras* allele alone (K14-CreER^{tam}/LSL-K-*ras*$^{G12D/+}$ mice; $P < 0.0001$). No animal death was observed in any of the control groups, including K14-CreER^{tam}, the *p53* deletion group (K14-CreER^{tam}/p53$^{F/F}$), and K14-CreER^{tam}/LSL-K-*ras*$^{G12D/+}$ mice treated with the vehicle. *Arrowhead,* initiation of the tamoxifen treatment. *C,* histopathology of the tongue carcinomas. An exophytic and infiltrative growth that covers most of the surface of the ventral and a part of the dorsal tongue is shown. Hyperkeratosis is evident even at this low magnification. Detail of the area depicted from *C* that shows the infiltrative border pushing downward into the connective tissue; at the cellular level, atypia is evident, with karyopyknosis, anisokaryosis, and focal dyskeratosis. Immunostaining for BrdUrd incorporation showing increased mitotic activity randomly distributed at all levels of the carcinomatous epithelium. K14 expression in the carcinomas shows positive staining in the upper layers. Isolated expression of K1 in the upper layers of the malignant proliferating squamous epithelium. Filaggrin expression was restricted to the upper layers. In control tongue, there is occasional BrdUrd incorporation and K14 expression in the basal layer, K1 is negative, and filaggrin is expressed in the upper layers.

by PCR analysis using oligonucleotides flanking the stop cassette (Fig. 2 and Supplementary Fig. S1). No recombination was observed in the absence of CreER^{tam} expression or tamoxifen induction, and LSL-K-*ras*^{G12D} allele recombination was readily demonstrable in K14-CreER^{tam}/LSL-K-*ras*$^{G12D/+}$ mice in the oral mucosa, tongue, and the papillomas arising in tamoxifen-treated mice (Fig. 2). LSL-K-*ras*^{G12D} allele recombination effectively occurred in the skin of K14-CreER^{tam}/LSL-K-*ras*$^{G12D/+}$ mice treated with tamoxifen (Supplementary Fig. S1), although these mice did not develop skin lesions (Supplementary Fig. S1). This is aligned with recent studies using a different keratinocyte-specific inducible Cre system in which mice did not develop skin malignancies unless persistently treated with phorbol esters as tumor promoter (23). Thus, in spite of *ras* being likely activated in many K14-expressing squamous epithelia in our animal system, these animals developed benign tumors only in the oral mucosa, suggesting that the oral epithelial cells might be particularly sensitive to *ras*-induced aberrant cell proliferation.

Excision of *p53* cooperates with *ras* to induce tongue carcinomas. *p53* is one of the most frequently mutated tumor suppressor gene in human malignancies (24). In HNSCC, mutations in *p53* occur in >50% of the oral cavity cancers and the presence of mutations that render *p53* functionally inactive is associated with tumor progression and decreased overall survival (25). Loss of heterozygosity of *p53* and inactivating mutations in its coding sequence or the accelerated destruction of its protein product, p53, by viral oncoproteins, such as by human papillomavirus E6, represents a common molecular alteration in HNSCC (3). Thus, to examine whether alterations in *p53* cooperate with *ras* during oral carcinogenesis, we bred the K14-CreER^{tam}/LSL-K-*ras*$^{G12D/+}$ mice with mice harboring a floxed allele of *p53* (14). Remarkably, these mice developed carcinomas on the tongue as early as 2 weeks after tamoxifen administration (Fig. 3*A*) and progressed into clearly visible carcinomas in only 3 weeks (Fig. 3) The concomitant activation of LSL-K-*ras*^{G12D} and deletion of the floxed p53 alleles

Published OnlineFirst May 12, 2009; DOI: 10.1158/0008-5472.CAN-08-4645

were confirmed by PCR analysis using DNA from these tumors (Supplementary Fig. S1).

The tumors were well-differentiated SCCs, with moderate cell atypia and focal dyskeratosis (Fig. 3). Dysplasias and microcarcinomas were also observed. Tongue carcinomas presented increased cell proliferation, with BrdUrd-positive cells distributed at all levels of the epithelium (Fig. 3). Unlike in the normal squamous epithelium, K14 expression was stronger in the upper layers in the carcinomatous epithelium (Fig. 3), similarly to that observed in *ras*-induced oral papillomas. K1 and filaggrin were expressed only in the upper layers of the malignant epithelium (Fig. 3). Interestingly, we observed a distinct susceptibility of tumor progression between the tongue and the oral mucosa. In contrast to the large SCC lesions in the tongue, the oral mucosa of the K14-CreER^{tam}/LSL-K-*ras*$^{G12D/+}$/*p53*$^{flox/flox}$ mice developed only squamous papillomas, with no signs of malignant transformation. Thus, the squamous epithelium of the tongue seems to be highly susceptible to *ras*-induced transformation but only when relieved from the tumor-suppressive activity of p53.

Molecular mechanisms contributing to *ras*-induced HNSCC progression. As expected, the carcinomas exhibited an elevated proliferative capacity, as judged by the increase in CCDN1 and PCNA staining (Fig. 4). The normal oral mucosa and tongue and their tumoral lesions all expressed K14, albeit with a distinct distribution pattern (see above). All papillomas expressed high levels of K1. This suggested that in all benign lesions, cell differentiation might restrain the oncogenic potential of *ras*. In contrast, in the absence of a functional *p53*, epithelial cells from the tongue may lose their ability to couple proliferation with differentiation, thereby resulting in malignant growth.

We next focused on the status of activation of the MAPK and Akt/mTOR pathway, two key signaling pathways activated by Ras (26, 27), by examining the levels of pMAPK and pS6, the most downstream target of the Akt/mTOR signaling route. We did not observe an increase in the level of pMAPK in *ras*-induced tumors, which is aligned with the observation that MAPK activation is not often observed in primary human HNSCC (28). This was confirmed by Western blot analysis of lysates from papillomas and carcinomas (Supplementary Fig. S2). By systematic analysis of potential events leading to MAPK inactivation in these cancer lesions, we found that *ras*-induced tumors overexpress a MAPK phosphatase, DUSP-14 (refs. 29, 30; Supplementary Fig. S2). Although the potential role of DUSP-14 in preventing MAPK activation is under current evaluation, the most remarkable finding in these tumors was a clear increase in

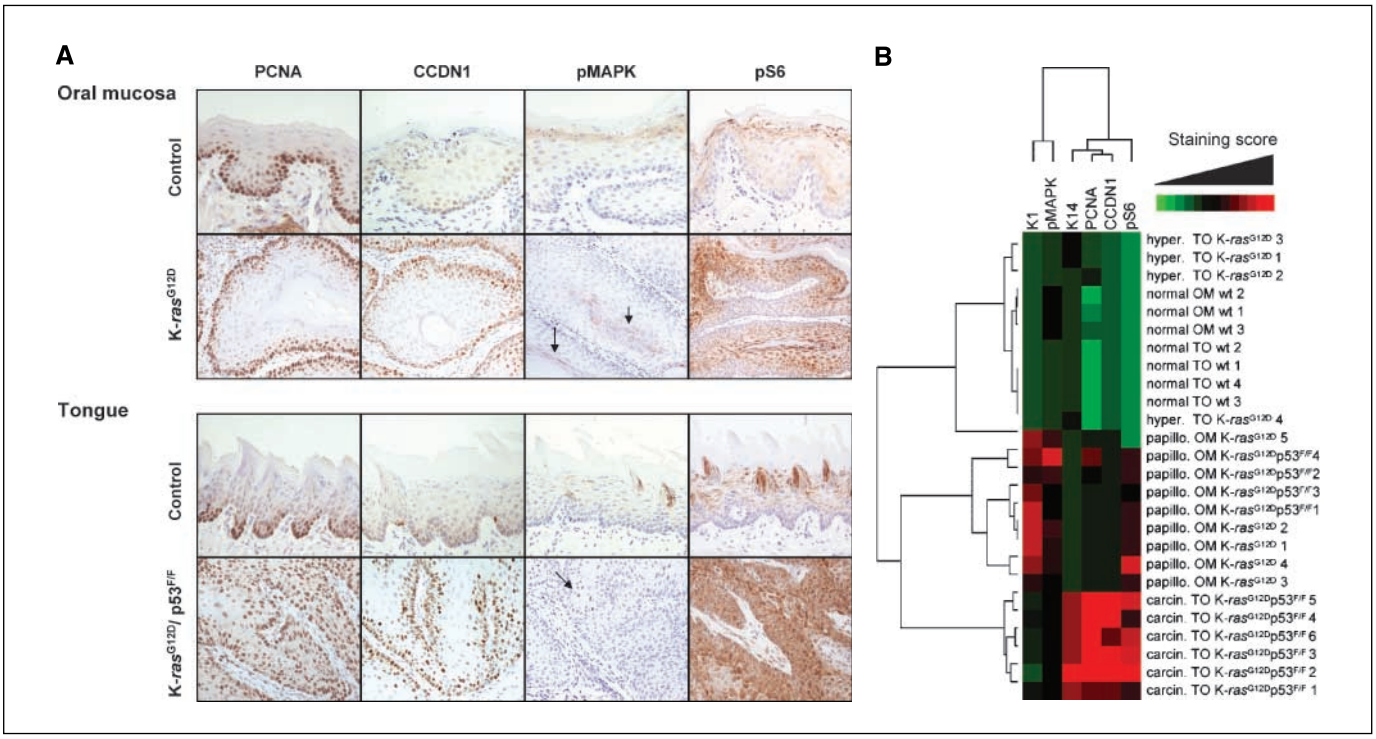

Figure 4. Immunohistochemical analysis of biomarkers in the oral mucosa and tongue lesions arising in the two-hit animal model. *A,* control oral mucosa: PCNA expression in normal mucosa shows positive reaction exclusively in the basal layer, and CCDN1 immunostaining revealed scattered mildly positive cells mainly in the basal layer. No staining with pMAPK is evident and low expression levels of pS6 are seen in the upper layers. Papillomas K-*ras*^{G12D}: PCNA immunoreaction is similar to that of the normal epithelium; CCDN1 shows a different staining pattern with many intensely and moderately stained cells in the basal layers. Papillomas show faint expression of pMAPK in few cells (*arrows*) in the more differentiated areas. Elevated pS6 immunoreactivity is observed in basal and intermediate layers of papillomas. Control tongue: PCNA expression in normal tongue is seen in the basal layer together with scattered and low-intensity CCDN1-positive cells. No evident staining for pMAPK is observed. pS6 immunoreactivity is located in the intermediate and upper layers. Carcinomas K-*ras*^{G12D} p53^{F}: the tongue carcinomas show increased mitotic activity reflected by a higher number of PCNA- and CCDN1-positive cells randomly distributed at all levels of the carcinomatous epithelium. *Arrow,* pMAPK detection is quite limited, showing only few positive cells. pS6 is highly expressed across all areas in tongue carcinomas. Original magnification, ×20. *B,* hierarchical clustering of immunohistochemical staining score for the different biomarkers studied. Tissues were classified based on the histology: normal, hyperplasia (*hyper.*), papilloma (*papillo.*), and carcinoma (*carcin.*). The collected samples were from oral mucosa (*OM*) and the tongue (*TO*). The genotypes were wild-type (*wt*), K14-CreER^{tam}/LSL-K-*ras*$^{G12D/+}$ (*K-ras*^{G12D}), and K14-CreER^{tam}/LSL-K-*ras*^{G12D}/p53$^{flox/flox}$ (*K-ras*^{G12D} *p53*$^{F/F}$). Numbers indicate individual animals. The clustered data were arranged with markers on the horizontal axis and tissue samples on the vertical axis. Biomarkers with a close relationship are located closer to each other. *Deep red,* high staining scores (strong staining intensity and 75–100% of positive-staining cells); *light green,* low staining scores (weak staining intensity and <25% of cells positive for immunohistochemistry). The accumulation of pS6, reflecting the activation of the mTOR pathway, correlated best with the malignant conversion from papilloma to carcinoma.

Published OnlineFirst May 12, 2009; DOI: 10.1158/0008-5472.CAN-08-4645

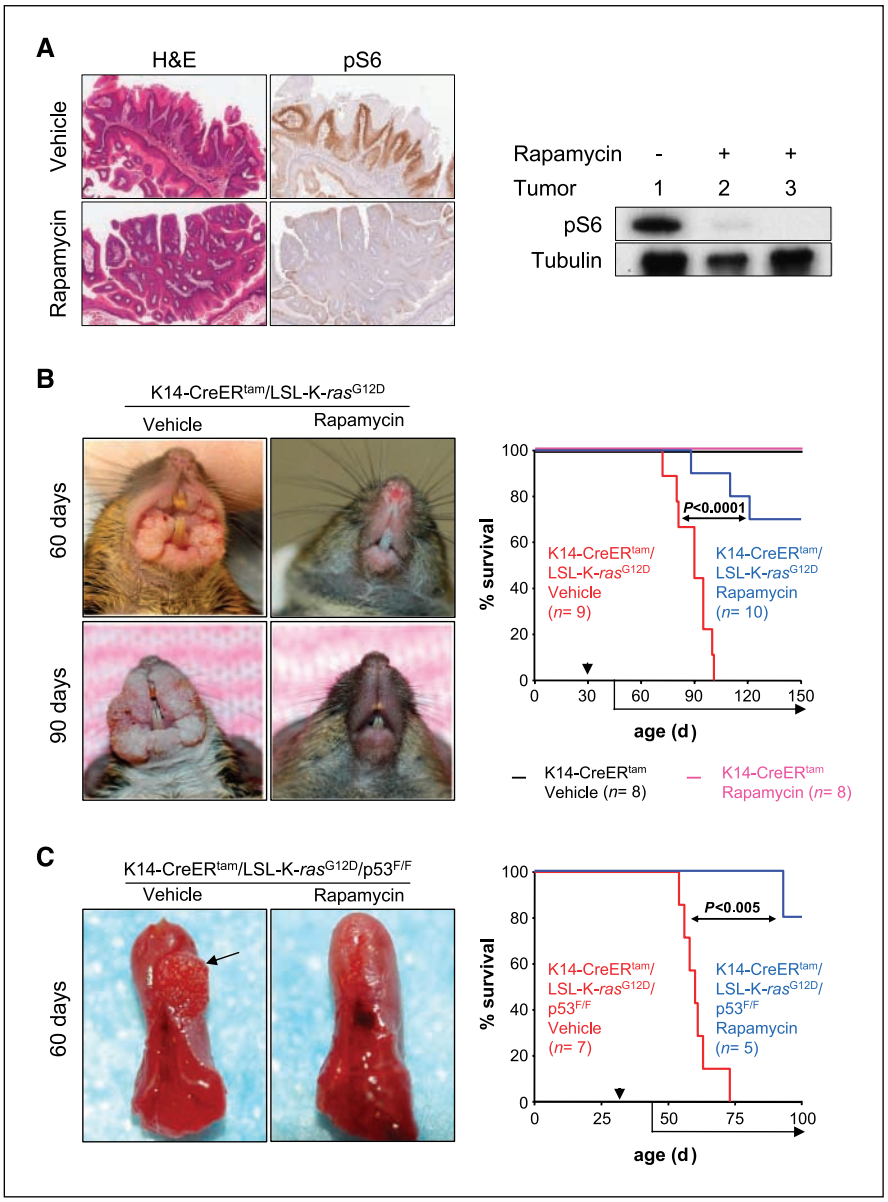

Figure 5. The K-*ras* and *p53* two-hit oral carcinogenesis model is dependent on mTOR. *A, left,* representative papillomas developed by K14-CreER^{tam}/LSL-K-*ras*$^{G12D/+}$ mice treated with rapamycin or vehicle for 3 consecutive days. The H&E histologic sections depict the typical features of the papillomas. Note the elevated level of pS6 in these tumors treated with vehicle in contrast with the remarkable reduction on rapamycin treatment. Original magnification, ×5. *Right,* Western blot analysis of pS6 in tumors treated with rapamycin. pS6 levels were examined in total cell lysates from papillomas developed in K14-CreER^{tam}/LSL-K-*ras*$^{G12D/+}$ mice treated with rapamycin or vehicle during 3 d. The high pS6 levels in control K14-CreER^{tam}/LSL-K-*ras*$^{G12D/+}$ mice are in contrast with the absence of pS6 in tumors treated with rapamycin. Tubulin was used as loading control. *B,* representative examples of K14-CreER^{tam}/LSL-K-*ras*$^{G12D/+}$ mice treated with rapamycin or vehicle as indicated. *Left,* papilloma development in a control mouse at the indicated age; *right,* K14-CreER^{tam}/LSL-K-*ras*$^{G12D/+}$ animal treated with rapamycin did not develop papillomas at the same age. Kaplan-Meier survival curve of the indicated mice lines treated or not with rapamycin. No animal death was observed in any of the control animal lines (see Fig. 3) treated with rapamycin or vehicle. The treatment of K14-CreER^{tam}/LSL-K-*ras*$^{G12D/+}$ mice with rapamycin prevented the development of oral papillomas and increased their life span when compared with vehicle control ($P < 0.0001$). *Arrowhead,* tamoxifen treatment. *Horizontal arrow,* beginning of the rapamycin or vehicle treatment that was started 1 wk after tamoxifen induction. *C, left,* representative tongues of K14-CreER^{tam}/LSL-K-*ras*$^{G12D/+}$/p53$^{flox/flox}$ mice treated with rapamycin or vehicle. *Left,* a tongue carcinoma (*arrow*) in a mouse of the control group at 60 d of age; *right,* K14-CreER^{tam}/LSL-K-*ras*$^{G12D/+}$/p53$^{flox/flox}$ animals treated with rapamycin did not develop tongue carcinomas at the same age. *Right,* Kaplan-Meier survival curve of the indicated mice lines treated or not with rapamycin. Rapamycin treatment of K14-CreER^{tam}/LSL-K-*ras*$^{G12D/+}$/p53$^{flox/flox}$ mice prevented the development of tongue carcinomas and increased their life span ($P < 0.005$). *Arrowhead* and *horizontal arrow,* treatments.

the level of pS6 in carcinomas and oral papillomas, which contrasts with the low level of pS6 in the normal tissues (Fig. 4).

The relationship between proliferative and differentiation markers and the activation of MAPK and the Akt/mTOR pathway was nicely reflected by the nonsupervised hierarchical class comparison of the immunostaining results (16), showing the existence of three well-defined clusters (Fig. 4). Control tissues grouped together, whereas hyperplasias and papillomas formed a separate group regardless of their genotype. All carcinomas defined a clearly distinct group, characterized by the increased expression of proliferative markers, PCNA and CCDN1, and basal keratins, K14, a reduced expression of suprabasal keratins, K1, and a remarkable accumulation of pS6. Indeed, the activation of the mTOR pathway correlated with the malignant conversion from papilloma to carcinoma, thus suggesting that the mTOR signaling route may contribute to carcinoma progression caused by the concomitant activation of *ras* and the inactivation of *p53* in the oral cavity.

Targeting mTOR halts the progression of K-*ras*–induced and *p53*-induced oral tumors. These observations, prior studies supporting that the activation of the Akt-mTOR pathway is a frequent event in HNSCC (15, 31–33), and the emerging use of mTOR inhibitors in cancer treatment (34) prompted us to explore whether interfering with mTOR signaling could prevent tumor development in this model. The treatment of mice harboring *ras*-induced tumors with rapamycin, a potent inhibitor of mTOR function (35), led to a dramatic decrease in pS6 levels in the tumoral lesions, as judged by immunohistochemical and Western blot analysis (Fig. 5). We next explored whether the development of these lesions was dependent on mTOR activation. For these studies, we induced Cre-mediated *ras* activation in animals harboring wild-type *p53* or its floxed allele by tamoxifen administration and, 1 week later, initiated the rapamycin treatment. The treatment of K14-CreER^{tam}/LSL-K-*ras*$^{G12D/+}$ mice with rapamycin prevented the development of oral tumors and increased their life span ($P < 0.0001$; Fig. 5). This was also clearly

observed in mice in which *ras* activation and p53 deletion led to squamous carcinomas. Indeed, rapamycin treatment prevented tumor progression and extended the life expectancy of these mice (Fig. 5).

Discussion

The combined inactivation of *p53* and activation of *ras* in a cellular compartment that includes the oral epithelial stem cells by the administration of tamoxifen to K14-CreER^{tam}/LSL-K-*ras*$^{G12D/+}$/p53$^{flox/flox}$ mice may provide a relevant two-hit animal model system resulting in the rapid development of oral squamous carcinomas in the tongue. This finding is consistent with the emerging notion that oral carcinomas arise from genetic alterations in the epithelial stem cell compartment (36). K14-CreER^{tam} also targets gene expression to self-renewing cells in other epithelial tissues, including the hair follicles and the interfollicular epithelium in the skin (12). However, activation of a single allele of *ras* and alterations in *p53* were unable to promote tumorigenesis in the skin, but sufficient for oral carcinogenesis, suggesting that different epithelial stem cells may harbor distinct transforming potential. There were even differences between the oral mucosa and the epithelium of the tongue. Whereas *ras* activation with or without *p53* inactivation caused the development of papillomas in the oral mucosa, *ras* alone caused only hyperproliferation of the epithelium of the tongue. However, *ras* activation and *p53* deletion resulted in the rapid development of squamous carcinomas exclusively in the tongue. This increased susceptibility to malignant conversion of the squamous epithelium of the tongue may explain the higher incidence of tongue HNSCC with respect to all other anatomic locations in the head and neck region (37) even if the exposure to carcinogens, such as those in tobacco, results in *p53* mutations in the epithelium lining the entire oropharynx (3).

This genetically defined HNSCC model system that does not require the use of tumor promoters affecting the stroma and connective tissue may now enable exploring the nature of the tumor cell autonomous molecular events driving SCC progression. Among them, the ability to uncouple epithelial cell proliferation with differentiation and the activation of the Akt-mTOR signaling pathway resulting in pS6 accumulation seem to represent early events in HNSCC progression (15, 16, 31–33). On the other hand, this model system enabled us to explore whether interfering with the activity of mTOR may represent a suitable approach to prevent or treat oral cancer. Indeed, we observed that decreasing mTOR activity by the administration of rapamycin after genetic recombination leading to *p53* deletion and *ras* activation was sufficient to prevent tumor progression. These findings, together with the recent observation that rapamycin causes the regression of SCC lesions caused by the classic two-step skin chemical carcinogenesis model (38) resulting from the accumulation of *ras* and *p53* mutations (38, 39), support the potential clinical benefit of targeting mTOR for the prevention and treatment of HNSCC, particularly in clinical cases that present premalignant and cancerous lesions harboring activated mutations in *ras*. Ultimately, the K14-CreER^{tam}/LSL-K-*ras*$^{G12D/+}$/p53$^{flox/flox}$ two-hit animal model system may represent a suitable platform for exploring the underlying molecular mechanism and genetic and epigenetic event determining the susceptibility to malignant progression of tumoral lesions arising from the distinct stratified epithelia of the oral cavity and may facilitate the development of new targeted approaches for the treatment and prevention of HNSCC.

Disclosure of Potential Conflicts of Interest

No potential conflicts of interest were disclosed.

Acknowledgments

Received 12/6/08; revised 3/15/09; accepted 3/25/09.

Grant support: Intramural Research Program of NIH, National Institute of Dental and Craniofacial Research.

The costs of publication of this article were defrayed in part by the payment of page charges. This article must therefore be hereby marked *advertisement* in accordance with 18 U.S.C. Section 1734 solely to indicate this fact.

We thank Drs. Maria L. Paparella and Kantima Leelahavanichkul for valuable advice and help.

References

1. Hashibe M, Brennan P, Benhamou S, et al. Alcohol drinking in never users of tobacco, cigarette smoking in never drinkers, and the risk of head and neck cancer: pooled analysis in the International Head and Neck Cancer Epidemiology Consortium. J Natl Cancer Inst 2007;99:777–89.
2. Jemal A, Siegel R, Ward E, et al. Cancer statistics, 2008. CA Cancer J Clin 2008;58:71–96.
3. Forastiere A, Koch W, Trotti A, Sidransky D. Head and neck cancer. N Engl J Med 2001;345:1890–900.
4. Kalyankrishna S, Grandis JR. Epidermal growth factor receptor biology in head and neck cancer. J Clin Oncol 2006;24:2666–72.
5. Saranath D, Chang SE, Bhoite LT, et al. High frequency mutation in codons 12 and 61 of H-ras oncogene in chewing tobacco-related human oral carcinoma in India. Br J Cancer 1991;63:573–8.
6. Hardisson D. Molecular pathogenesis of head and neck squamous cell carcinoma. Eur Arch Otorhinolaryngol 2003;260:502–8.
7. Lu SL, Herrington H, Reh D, et al. Loss of transforming growth factor-β type II receptor promotes metastatic head-and-neck squamous cell carcinoma. Genes Dev 2006;20:1331–42.
8. Frese KK, Tuveson DA. Maximizing mouse cancer models. Nat Rev Cancer 2007;7:645–58.
9. Vitale-Cross L, Amornphimoltham P, Fisher G, Molinolo AA, Gutkind JS. Conditional expression of K-ras in an epithelial compartment that includes the stem cells is sufficient to promote squamous cell carcinogenesis. Cancer Res 2004;64:8804–7.
10. Raimondi AR, Vitale-Cross L, Amornphimoltham P, Gutkind JS, Molinolo A. Rapid development of salivary gland carcinomas upon conditional expression of K-ras driven by the cytokeratin 5 promoter. Am J Pathol 2006;168:1654–65.
11. Caulin C, Nguyen T, Longley MA, Zhou Z, Wang XJ, Roop DR. Inducible activation of oncogenic K-ras results in tumor formation in the oral cavity. Cancer Res 2004;64:5054–8.
12. Vasioukhin V, Degenstein L, Wise B, Fuchs E. The magical touch: genome targeting in epidermal stem cells induced by tamoxifen application to mouse skin. Proc Natl Acad Sci U S A 1999;96:8551–6.
13. Jackson EL, Willis N, Mercer K, et al. Analysis of lung tumor initiation and progression using conditional expression of oncogenic K-ras. Genes Dev 2001;15:3243–8.
14. Jonkers J, Meuwissen R, van der Gulden H, Peterse H, van der Valk M, Berns A. Synergistic tumor suppressor activity of BRCA2 and p53 in a conditional mouse model for breast cancer. Nat Genet 2001;29:418–25.
15. Amornphimoltham P, Patel V, Sodhi A, et al. Mammalian target of rapamycin, a molecular target in squamous cell carcinomas of the head and neck. Cancer Res 2005;65:9953–61.
16. Molinolo AA, Hewitt SM, Amornphimoltham P, et al. Dissecting the Akt/mammalian target of rapamycin signaling network: emerging results from the head and neck cancer tissue array initiative. Clin Cancer Res 2007;13:4964–73.
17. Vassar R, Rosenberg M, Ross S, Tyner A, Fuchs E. Tissue-specific and differentiation-specific expression of a human K14 keratin gene in transgenic mice. Proc Natl Acad Sci U S A 1989;86:1563–7.
18. Barbacid M. ras genes. Annu Rev Biochem 1987;56:779–827.
19. Bos JL. ras oncogenes in human cancer: a review. Cancer Res 1989;49:4682–9.
20. Nunez F, Dominguez O, Coto E, Suarez-Nieto C, Perez P, Lopez-Larrea C. Analysis of ras oncogene mutations in human squamous cell carcinoma of the head and neck. Surg Oncol 1992;1:405–11.
21. Anderson JA, Irish JC, McLachlin CM, Ngan BY. H-ras oncogene mutation and human papillomavirus infection in oral carcinomas. Arch Otolaryngol Head Neck Surg 1994;120:755–60.
22. Roop DR, Krieg TM, Mehrel T, Cheng CK, Yuspa SH. Transcriptional control of high molecular weight keratin gene expression in multistage mouse skin carcinogenesis. Cancer Res 1988;48:3245–52.
23. Caulin C, Nguyen T, Lang GA, et al. An inducible

Published OnlineFirst May 12, 2009; DOI: 10.1158/0008-5472.CAN-08-4645

mouse model for skin cancer reveals distinct roles for gain- and loss-of-function p53 mutations. J Clin Invest 2007;117:1893–901.

24. Vousden KH, Lane DP. p53 in health and disease. Nat Rev Mol Cell Biol 2007;8:275–83.

25. Poeta ML, Manola J, Goldwasser MA, et al. TP53 mutations and survival in squamous-cell carcinoma of the head and neck. N Engl J Med 2007;357:2552–61.

26. Sebolt-Leopold JS, Herrera R. Targeting the mitogen-activated protein kinase cascade to treat cancer. Nat Rev Cancer 2004;4:937–47.

27. Sabatini DM. mTOR and cancer: insights into a complex relationship. Nat Rev Cancer 2006;6:729–34.

28. Albanell J, Codony-Servat J, Rojo F, et al. Activated extracellular signal-regulated kinases: association with epidermal growth factor receptor/transforming growth factor α expression in head and neck squamous carcinoma and inhibition by anti-epidermal growth factor receptor treatments. Cancer Res 2001;61:6500–10.

29. Marti F, Krause A, Post NH, et al. Negative-feedback regulation of CD28 costimulation by a novel mitogen-activated protein kinase phosphatase, MKP6. J Immunol 2001;166:197–206.

30. Boutros T, Chevet E, Metrakos P. Mitogen-activated protein (MAP) kinase/MAP kinase phosphatase regulation: roles in cell growth, death, and cancer. Pharmacol Rev 2008;60:261–310.

31. Amornphimoltham P, Sriuranpong V, Patel V, et al. Persistent activation of the Akt pathway in head and neck squamous cell carcinoma: a potential target for UCN-01. Clin Cancer Res 2004;10:4029–37.

32. Massarelli E, Liu DD, Lee JJ, et al. Akt activation correlates with adverse outcome in tongue cancer. Cancer 2005;104:2430–6.

33. Molinolo AA, Amornphimoltham P, Squarize CH, Castilho RM, Patel V, Gutkind JS. Dysregulated molecular networks in head and neck carcinogenesis. Oral Oncol. Epub 2008 Sept 18.

34. Guertin DA, Sabatini DM. Defining the role of mTOR in cancer. Cancer Cell 2007;12:9–22.

35. Sabers CJ, Martin MM, Brunn GJ, et al. Isolation of a protein target of the FKBP12-rapamycin complex in mammalian cells. J Biol Chem 1995;270:815–22.

36. Hunter KD, Parkinson EK, Harrison PR. Profiling early head and neck cancer. Nat Rev Cancer 2005;5: 127–35.

37. Shiboski CH, Schmidt BL, Jordan RC. Tongue and tonsil carcinoma: increasing trends in the U.S. population ages 20-44 years. Cancer 2005;103:1843–9.

38. Amornphimoltham P, Leelahavanichkul K, Molinolo A, Patel V, Gutkind JS. Inhibition of mammalian target of rapamycin by rapamycin causes the regression of carcinogen-induced skin tumor lesions. Clin Cancer Res 2008;14:8094–101.

39. Balmain A, Pragnell IB. Mouse skin carcinomas induced *in vivo* by chemical carcinogens have a transforming Harvey-ras oncogene. Nature 1983;303:72–4.

Cancer Research
The Journal of Cancer Research (1916–1930) | The American Journal of Cancer (1931–1940)

AACR American Association for Cancer Research

Rapamycin Prevents Early Onset of Tumorigenesis in an Oral-Specific K-*ras* and *p53* Two-Hit Carcinogenesis Model

Ana R. Raimondi, Alfredo Molinolo and J. Silvio Gutkind

Cancer Res 2009;69:4159-4166. Published OnlineFirst May 12, 2009.